REPORT DOCUMENTATION PAGE

Form Approved OMB NO. 0704-0188

1. REPORT DATE (DD-MM-YYYY)	2. REPORT TYPE	3. DATES COVERED (From - To)
17-08-2012	Conference Proceeding	-

4. TITLE AND SUBTITLE

Designing Alkaline Exchange Membranes from Scratch

5a. CONTRACT NUMBER
W911NF-10-1-0520

5b. GRANT NUMBER

5c. PROGRAM ELEMENT NUMBER
611103

6. AUTHORS

Yushan Yan, Gregory A. Voth, Thomas A. Witten, Matthew W. Liberatore, Andrew M. Herring, Melissa A. Vandiver, Ashley M. Maes, Himanshu Sarode, Benjamin Caire, James L. Horan, Yating Yan, Yifan

5d. PROJECT NUMBER

5e. TASK NUMBER

5f. WORK UNIT NUMBER

7. PERFORMING ORGANIZATION NAMES AND ADDRESSES

Colorado School of Mines
Colorado School of Mines
1500 Illinois Street
Golden, CO 80401 -

8. PERFORMING ORGANIZATION REPORT NUMBER

9. SPONSORING/MONITORING AGENCY NAME(S) AND ADDRESS(ES)

U.S. Army Research Office
P.O. Box 12211
Research Triangle Park, NC 27709-2211

10. SPONSOR/MONITOR'S ACRONYM(S)
ARO

11. SPONSOR/MONITOR'S REPORT NUMBER(S)
58161-CH-MUR.10

12. DISTRIBUTION AVAILIBILITY STATEMENT

Approved for public release; distribution is unlimited.

13. SUPPLEMENTARY NOTES

The views, opinions and/or findings contained in this report are those of the author(s) and should not contrued as an official Department of the Army position, policy or decision, unless so designated by other documentation.

14. ABSTRACT

There is increasing interest in the alkaline exchange membrane (AEM) fuel cells as this device, if realized, could allow the use of inexpensive metal catalysts and the oxidation of a variety of convenient liquid fuels. While there have been some dramatic early achievements, there is still a need for a fundamental study of

15. SUBJECT TERMS

Anion Exchange Membrane; Fuel Cell; anion conduction

16. SECURITY CLASSIFICATION OF:			17. LIMITATION OF ABSTRACT	15. NUMBER OF PAGES	19a. NAME OF RESPONSIBLE PERSON
a. REPORT	b. ABSTRACT	c. THIS PAGE			Andrew Herring
UU	UU	UU	UU		19b. TELEPHONE NUMBER: 303-384-2082

Report Title

Designing Alkaline Exchange Membranes from Scratch

ABSTRACT

There is increasing interest in the alkaline exchange membrane (AEM) fuel cells as this device, if realized, could allow the use of inexpensive metal catalysts and the oxidation of a variety of convenient liquid fuels. While there have been some dramatic early achievements, there is still a need for a fundamental study of anion transport, cation stability and the formation of robust thin films in this area. We have undertaken a comprehensive study of AEMs where theory is linked to well-defined model systems, both in solution and in the solid state, which are characterized using very careful environmental control such that the models can be validated and used predictively. We are also fabricating a number of random copolymer AEMs that can be produced readily in large quantities, allowing us to understand film formation coupled with transport and stability. Those based on perfluorinated backbones invite interesting comparisons with the analogous proton exchange membranes.

Conference Name: 220th ECS Meeting

Conference Date: October 10, 2011

Designing Alkaline Exchange Membranes from Scratch

Himanshu Sarode, Melissa A. Vandiver, Ashley M. Maes, Benjamin Caire, James L. Horan, Yating Yan, Yifan Li, Gerrick E. Lindberg, James F. Dama, Chris Knight, Ryan Jorn, Martin E. Lenz, Robert Kasper, Shuang Gu, Bingzi Zhang, Sönke Seifert, Tsung-han Tsai, Wen X. Zhang, E. Bryan Coughlin, Daniel M. Knauss, Yushan Yan, Gregory A. Voth, Thomas A. Witten, Matthew W. Liberatore and Andrew M. Herring

ECS Trans. 2011, Volume 41, Issue 1, Pages 1761-1774.
doi: 10.1149/1.3635708

ECS Transactions, 41 (1) 1761-1774 (2011)
10.1149/1.3635708 ©The Electrochemical Society

Designing Alkaline Exchange Membranes from Scratch.

Himanshu Sarode,[a] Melissa A. Vandiver,[a] Ashley M. Maes,[a] Benjamin Caire,[a] James L. Horan,[a] Yating Yang,[b] Yifan Li,[b] Gerrick E. Lindberg,[e] James F. Dama,[e] Chris Knight,[e] Ryan Jorn,[e] Martin E. Lenz,[f] Robert Kaspar,[d] Shuang Gu,[d] Bingzi Zhang,[d] Sönke Seifert,[g] Tsung-han Tsai,[c] WenXu Zhang,[c] E. Bryan Coughlin,[c] Daniel M. Knauss,[b] Yushan Yan,[d] Gregory A. Voth,[e] Thomas A. Witten,[f] Matthew W. Liberatore,[a] and Andrew M. Herring,[a]

[a] Department of Chemical Engineering and
[b]Department of Chemistry and Geochemistry, Colorado School of Mines, Golden, CO 80401, USA
[c]Department of Polymer Science and Engineering, Conte Research Center, University of Massachusetts, Amherst, MA 01003, USA
[d]Department of Chemical Engineering, University of Delaware, Newark, DE 19716, USA
[e]Department of Chemistry and [f]Department of Physics, James Franck Institute and Computation Institute, University of Chicago, Chicago, IL 60637, USA
[g]Advanced Photon Source, Argonne National Laboratory, Argonne, Illinois, 60439, USA

There is increasing interest in the alkaline exchange membrane (AEM) fuel cells as this device, if realized, could allow the use of inexpensive metal catalysts and the oxidation of a variety of convenient liquid fuels. While there have been some dramatic early achievements, there is still a need for a fundamental study of anion transport, cation stability and the formation of robust thin films in this area. We have undertaken a comprehensive study of AEMs where theory is linked to well-defined model systems, both in solution and in the solid state, which are characterized using very careful environmental control such that the models can be validated and used predictively. We are also fabricating a number of random copolymer AEMs that can be produced readily in large quantities, allowing us to understand film formation coupled with transport and stability. Those based on perfluorinated backbones invite interesting comparisons with the analogous proton exchange membranes.

Introduction

While there has been much interest in the proton exchange membrane (PEM) fuel cell, its widespread use has been restricted by cost, durability, and fuel versatility issues. This is primarily because Pt is the catalyst of choice for a PEM fuel cell on both the anode and the cathode. Alkaline catalysis in fuel cells has been demonstrated with non-precious metal catalysts (1), and with a variety of fuels beyond H_2 and methanol. Alkaline fuel cells (AFCs), based on aqueous solutions of KOH, have serious drawbacks associated with system complexity and carbonate formation. Anion exchange membrane (AEMs) fuel cells have a number of advantages over both PEM fuel cells and traditional AFCs;

however, ionic conductivity in AEMs is significantly lower than PEMs and chemical stability of membrane cations in hydroxide has been poor (2).

It is important to reiterate the requirements for end use of AEMs for fuel cell applications in considering synthetic design at the molecular level. The membranes obviously must have high hydroxide (and carbonate) conductivity and low electronic conductivity, but must also be chemically, dimensionally, and mechanically stable at elevated temperatures, under a range of hydration conditions, and using potentially different fuels. Utilizing a wealth of background literature, our synthetic expertise, and the guidance from team members employing advanced theory and computation, we are iteratively designing AEM from both a molecular and practical perspective.

Theory

Work in the Voth group is comprised of developing integrated, multiscale models capable of predicting the hydroxide conductivity of polymer anion exchange membranes (AEMs) using only the chemical formula of the polymers and morphology information from experiments (Figure 1). First, *ab initio* molecular dynamics (AIMD) simulations were used to accurately model hydroxide ions in aqueous solution and in AEMs. Next, we employed reactive molecular dynamics to study hydroxides interacting with polymers in fully atomistic AEM pore microenvironments. Lastly, nonequilibrium continuum simulations were used to understand hydroxide transport through explicitly incorporated complex, heterogeneous pore networks on the macroscale. These correspond to the ionic scale, the pore scale, and the network scale, respectively, and together they bridge the gap between chemical formula and bulk transport properties.

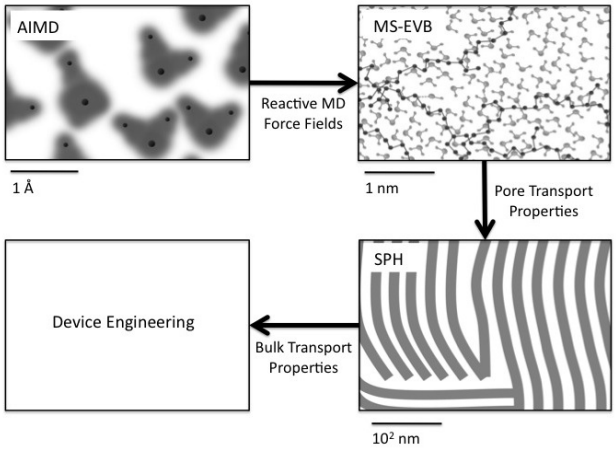

Figure 1. A schematic representation of the multiscale strategy employed by the Voth group. Each method selected is able to model the system accurately and efficiently at the scale desired.

The first among these models employ AIMD to calculate hydroxide solvation and diffusion properties directly from quantum mechanics. AIMD simulations are able to accurately describe the changing chemical bond arrangements important for aqueous transport of hydroxide ions. These AIMD simulations are able to capture both the vehicular and proton jumping (Grotthuss) contributions to diffusion, while standard

classical molecular dynamics simulations only describe vehicular diffusion because they are restricted to a fixed bonding topology defined at the beginning of the simulation. If care is taken to select the appropriate density functional theory, then the hydroxide ion solvation and dynamic properties are found to be consistent with experiment (3), similar to our analogous studies of the hydrated excess proton (4). We have employed AIMD to model the hydroxide ion in concentrated solutions and in small sections of representative regions of model AEMs. The simulations of concentrated hydroxide solutions shed light on the fundamental transport mechanisms governing the diffusion of hydroxide in water. Meanwhile, the AIMD simulations of AEMs provide information to validate the reactive force fields used in pore-scale simulations and to contribute to fundamental understanding of the effects of confinement on hydroxide solvation and transport.

At the pore scale, AEM systems are modeled using the multi-state empirical valence bond (MS-EVB) method, a multiconfigurational molecular dynamics (MD) method able to efficiently and accurately describe bond making and breaking processes. These models are used to simulate hydroxide ion solvation and transport in the complex AEM pore microenvironment. While MS-EVB models do not exactly reproduce the performance of AIMD simulations, they can capture the changing bond topology, and therefore capture Grotthuss shuttling of the hydroxide ion. The AEM pore structure is prepared for various relevant morphologies using experimental data to ensure that the models correspond to realistic polymer configurations since the longest relaxation times in AEMs are currently beyond the range of atomistic MD simulations. These MS-EVB simulations are parameterized using information from AIMD and experiment and provide detailed insight into the transport mechanism of concentrated hydroxide in the membrane pore microenvironment. Work is ongoing to explore the relationship between Grotthuss shuttling and vehicular diffusion in AEMs, in particular to clarify the role of anti-correlated motion of charge. These simulations are being used to understand the roll of water content in hydroxide transport and AEM performance. As previously discussed, the ion transport mechanism can be decomposed into standard vehicular and Grotthuss hopping components. These components were found to be anti-correlated in Nafion^{TM} (5) and it remains unclear if hydroxide transport in AEMs is similar, or what design parameters may influence this effect. The data from these simulations contributes to the fundamental understanding of hydroxide solvation and transport in confined, polyelectrolyte pervaded environments.

To understand macroscopic hydroxide diffusion through AEMs, on the scale of the pore network, a different approach is needed. The work here focuses on AEMs with pores characterized by a smallest length scale that is large compared to the size of a solvated hydroxide ion, so that ion transport through these domains may be well approximated by a continuum model. The continuum models are parameterized by data from the MS-EVB simulations and experimental morphology data and then solved approximately using the particle-based method, smoothed-particle hydrodynamics (SPH), which is a natural choice for systems with advection and complicated, potentially moving boundary conditions. The SPH approach projects the continuum model onto a discrete set of overlapping mass elements which advect with the local solution flow and exchange momentum and component concentrations to satisfy viscous and diffusive transport laws, effectively discretizing the Langrangian formulation of the usual transport equations (6). This approach has been applied to simulate lipid vesicles (7), demonstrating that the method is capable of capturing coupled elastic, viscous, and diffusive behavior, all of

which may play a role in AEM transport at the pore network scale, even near to sharp interfaces, which are also present in AEMs. No satisfactory prediction of bulk transport properties from local transport properties has yet been made for polymer electrolyte membranes (8), so a deeper understanding of transport at the macroscale is essential to understand the connection of local transport properties and mechanistic insight provided by the pore scale MS-EVB models to larger scale phenomena.

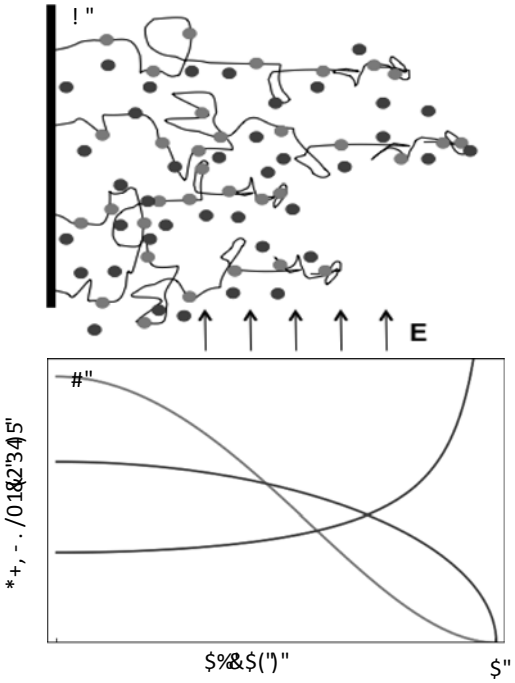

Figure 2. A) Sketch of a polymer brush showing polymer-bound ions (light dots) mobile counterions (dark dots) flexible, linear chains (black lines) and a transverse electric field that would drive a transverse current. B) Profiles of conductivity σ(z) normalized to give equal total conductances with various values of exponents μ_1 and m_1. Upper line at left corresponds to $\mu_1 = m_1 = 1$; middle line, $\mu_1 = 1$, $m_1 = -1/2$; lower line, $\mu_1 = 1$, $m_1 = -3/2$.

In Nafion™ the characteristic size of a pore and the distance between pores is around five nanometers, i.e., tens of water diameters. The aqueous pores contain polymer-bound ions and monomers as well as water and water-derived cations. A commonly-used water-to-ion ratio, λ, is about five. If a cation is the same volume as a water molecule, the volume fraction of water within the pore is only 80 percent. If one counts the bound ions and the coexisting monomers, the water volume fraction can only decrease. Concentrated environments like this typically give rise to large effects on free ion concentration and on the mobile ions' mobility. The same is to be expected for the anionic exchange membranes studied in the MURI. Matters are made more complicated since these compositional features are expected to vary strongly across a given pore. This variation approaches a mesoscopic scale amenable to continuum description.

In order to study how transport may be affected by these pore-scale variations, we have focused on a simple geometry that is at once calculable and experimentally implementable with diblock polymers such as those being synthesized by Coughlin and Knauss as part of the MURI. We imagine casting a monolayer of the diblocks on a hydrophobic surface and then hydrating the exposed hydrophilic blocks to form a polymer brush

(Figure 2a). The degree of hydration is experimentally controllable. Such a brush displays the same range of local environments expected in the pore space of realistic membranes. The proximal region near the grafted diblock interface is concentrated in monomers; the distal region is dilute. Conduction transverse to the brush corresponds to conduction through a pore. Each slab of the brush at a given height z makes its own contribution $\sigma(z)$ to this transverse conductance. This $\sigma(z)$ in turn is the product of the mobile ion density $c_i(z)$ and the ion mobility $m(z)$. Finally, the mobility depends on z via the local monomer concentration $c(z)$. How m depends on concentration c is subject to the atomic-scale steric and bonding constraints determined by Voth group simulations. For a given equation-of-state function relating the monomer chemical potential μ to monomer concentration c, one may determine the concentration profile $c(z)$ and thence $c_i(z)$, $m(c(z))$ and finally the conductivity $\sigma(z)$. It is not clear at the outset whether σ should have an important dependence on height z. Neither is it obvious whether the dense proximal region or the dilute distal region favors conduction more. The proximal region offers high ion concentration but potentially low mobility, so the net effect on σ is not clear. Yet one must have a good understanding of this point in order to optimize the anion-transport membrane. At present we lack the needed input information about $\mu(c)$ and $m(c)$ to answer this question. Nevertheless, we can provide an exploratory picture of the possibilities. We have recently formulated such a picture (9). In order to explore a range of behavior of $\mu(c)$ and $m(c)$, he takes these functions to have a power-law form with constants of proportionality μ_0, m_0 and c_0, and exponents μ_1 and m_1: $\mu(c)= \mu_0(c/c_0)^{\mu 1}$ and $m(c)= m_0(c/c_0)^{m1}$. In this initial work Witten has ignored the distinction between the local ion concentration c_i and the monomer concentration c. These powers are empirical constructs to be applied in limited ranges of concentration.

In concentrated polymer solutions, $\mu(c)$ follows an approximate power law with an exponent μ_1 in the range of 2. On the other hand, measurements (10) suggest a mobility falling rapidly with increasing concentration. This can be approximated using an m_1 in the range of -4. In order to determine the needed dependence on height z, one must take account of the equilibrium relationship between the stretching energy of the polymer chains in the brush and the chemical potential gradient $d\mu/dz$. The result is a simple quadratic dependence of μ on height z: $\mu = \mu_0(1 - (z/h)^2)$, where h is the height of the brush (11).

Given these conditions one may deduce the height dependence of conductivity σ for different assumed values of the exponents m_1 and μ_1. Some sample results are pictured in Figure 2b. As anticipated, a strong inverse dependence of mobility on concentration leads to conductivity, and thence current predominantly in the distal region.

These schematic results give a hint of what one might expect for a real brush. With experimental input replacing the empirical power laws, one can expect refined predictions of the conductivity profile and the resulting conductance as a function of molecular weight, grafting density and degree of hydration. In this way, one can seek to avoid large regions of hindered mobility or un-needed dilution and thereby maximize the conductivity of the brush as a whole.

Polymer synthesis

Block copolymers can self-assemble to provide versatile platforms for the fabrication of nanostructure materials with a wide range of morphologies such as cylinders, lamellae and gyroids. Polymer membranes made from block copolymers with one charged block can provide well-defined and continuous microdomains to enhance ion conductivity for use in fuel cells. The mechanical strength of the membranes could be improved because of the presence of a hydrophobic domain in the block copolymer. Balancing of the characteristics of these amphiphilic block copolymers is critical to developing robust membrane materials. Adopting key findings from investigations by Voth and Witten is guiding our synthetic choices for the identity of the cationic moiety incorporated by our tailored synthetic approaches. Their results from reactive molecular dynamics investigations help us in understanding the interaction of solvated hydroxide ions with the corresponding counter-cationic charges of the block copolymer. The morphologies adopted by the amphiphilic block copolymers are being investigated by both scattering experimentation in conjunction with Herring and electron microscopy investigations are planned with F. Beyer at ARL. The structural analysis findings from these investigations will be compared with the nonequilibrium continuum simulations by Voth to more completely understand hydroxide transport through heterogeneous pore networks on the macroscale.

The Coughlin group has synthesized polystyrene-*block*-poly (vinylbenzyltrimethylammonium tetrafluoroborate) (PS-*b*-[PVBTMA][BF_4]) via sequential atom transfer radical polymerization (ATRP) of styrene and vinyl-3/4-benzyl trimethyl ammonium tetrafluoroborate. Polystyrene-*b*-poly (vinylbenzyltrimethylammonium hydroxide) (PS-*b*-[PVBTMA][OH]) was subsequently prepared by ion exchange with hydroxide. Membranes of the block copolymers were made by drop casting from dichloromethane, initial evaluation of the microphase separation in block copolymers reveals the formation of hydrophilic [PVBTMA][BF_4] domains and hydrophobic PS domains.

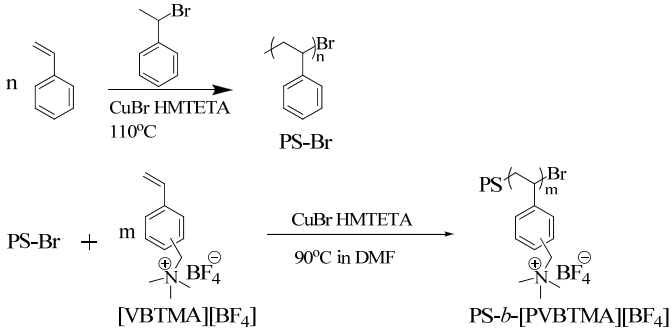

Scheme 1. Synthesis of PS-*b*-[PVBTMA][BF_4]

Small angle X-ray scattering experiments were performed to determine the morphology of PS-*b*-[PVBTMA][BF_4] membranes at different composition between two blocks. SAXS data (log (I) vs q) for the PS-*b*-[PVBTMA][BF_4] membranes casted from dichloromethane is shown in Figure 3. SAXS data of sample PS-*b*-[PVBTMA][BF_4]-1 is shown in figure 3(a), the existence of one distinct reflection at q equals to 0.43 nm^{-1} with d-spacing about 14.5 nm indicates poor defined morphology. For sample PS-*b*-[PVBTMA][BF_4]-2, the SAXS data (figure 3(b)) shows reflections at q and 2q which is indicative of a lamellar morphology with d-spacing 45.8 nm. The larger d-spacing of

sample PS-*b*-[PVBTMA][BF_4]-2 compared to sample PS-*b*-[PVBTMA][BF_4]-1 is expected due to the higher M_n of the starting PS block.

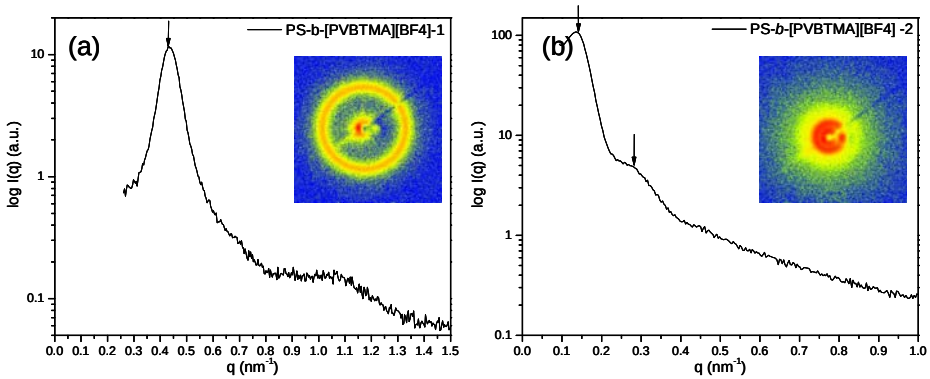

Figure 3. SAXS profiles for PS-*b*-[PVBTMA][BF_4] membranes.

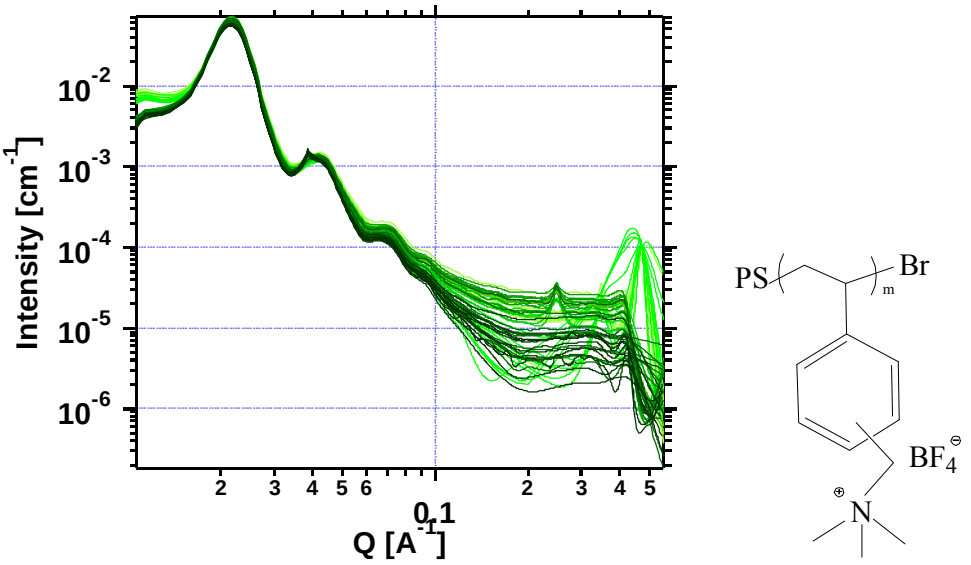

Figure 4. SAXS at 80°C from 25%RH, light, to 100%RH, dark with the polymer shown on the right with a M_n = 15.6 kg/mol, recorded at the APS.

In Figure 4 we show how the SAXS pattern changes at 80°C, a rather aggressive temperature for a novel AEM, from 25%RH to 100%RH. Clearly the morphology changes as the peaks at 0.022 and 0.055 $Å^{-1}$ collapse while the peak at 0.45 $Å^{-1}$ shows swelling due to the increased humidity. It is not known at this time whether these changes are reversible.

An inherent limitation of the use of polystyrene for the hydrophobic block is its high glass transition temperature and brittle nature. We have modified our synthetic approach to incorporate either polyisoprene, or after hydrogenation, an alternating poly(methyl butylene) hydrophobic block. Scheme 2 illustrates the sequential reaction we have developed to form amphiphilic block copolymers in which the hydrophobic block is now a low glass transition temperature amorphous block. An added advantage of this synthetic route is that the chemical composition, and morphology of the neutral copolymer precursor poly(4-methyl styrene-*b*- methyl butylene) P(4MS-*b*-PMB) can be

fully characterized by standard polymer characterization techniques and does not suffer from the associated difficulties in the characterization of polyelectrolytes, or amphiphilic copolymers.

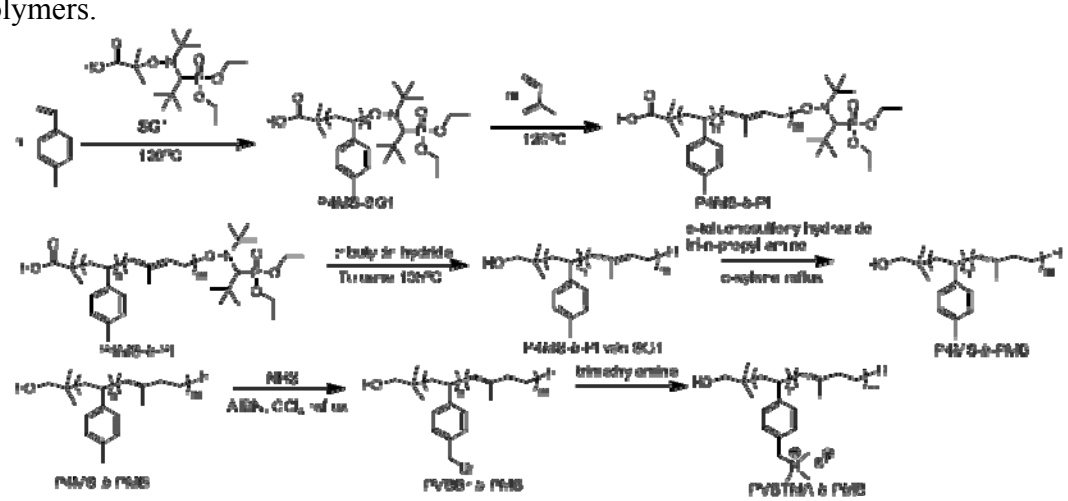

Scheme 2. Synthesis of PMB-*b*-[PVBTMA][Br]

Similar to the synthetic work described above, research in the Knauss group is proceeding to produce different functional block copolymers through combinations of anionic polymerization and nitroxide mediated radical polymerization. Anionically polymerized polybutadiene is produced with high 1,4-content and then converted to a nitroxide functional chain end by substitution with 2,2,6,6-tetramethyl-1-(2-bromo-1-phenylethoxy) piperidine. The nitroxide functional macroinitiator is used to polymerize a mixture of 3 and 4 isomers of vinylbenzyl chloride to produce a block of poly(vinylbenzyl chloride). The block copolymer can be solution cast into films and then reacted with trimethylamine to convert the benzyl chloride pendent groups into benzyltrimethylammonium groups, making polybutadiene-*block*-poly(vinylbenzyltrimethylammonium chloride) (PB-*b*-PVBTMA [Cl]). The advantage of the anionically polymerized butadiene with high 1,4 content is that hydrogenation can also be done to produce a polyethylene block that has high crystallinity. After hydrogenation, the resulting polyethylene-*block*-poly(vinylbenzyl chloride) can be solution cast and reacted with trimethylamine to make films of PE-*b*-PVBTMA [Cl]. The synthesis procedure is depicted in Scheme 3.

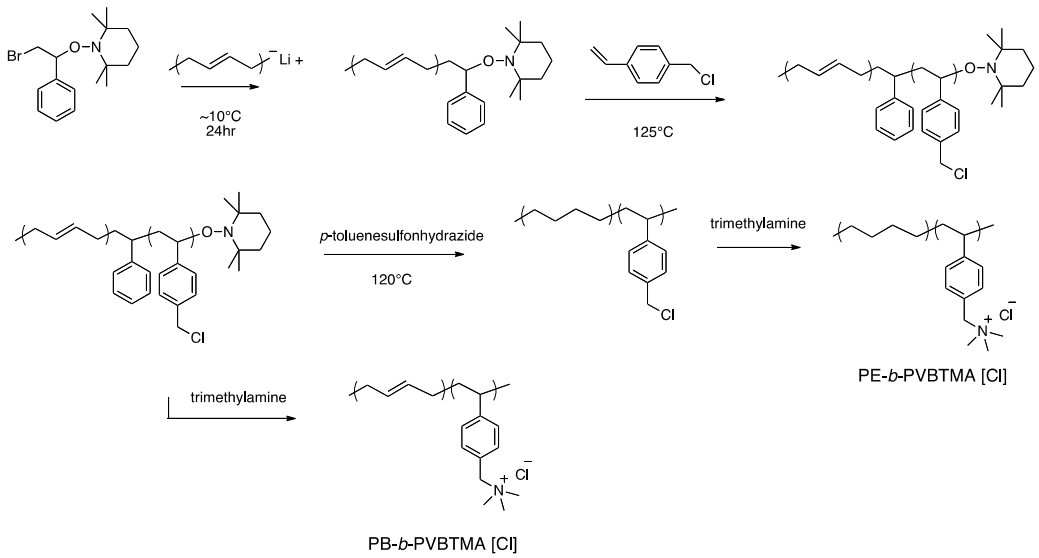

Scheme 3. Synthesis of PB-*b*-PVBTMA[Cl], and PE-*b*-PVBTMA[Cl]

With the different compositions of PS-*b*-[PVBTMA], PMB-*b*-[PVBTMA] , PB-*b*-PVBTMA, and PE-*b*-PVBTMA amphiphilic block copolymers, we will be able to test experimentally the theories of Witten on how transport may be affected by pore-scale variations. Casting of monolayers on a hydrophobic surface, for example polystyrene or polyethylene, and then selectively hydrating the ionic block will allow us to probe conduction of the corresponding counter anions transverse to the extend brush structures. With experimental measurements we anticipate being able to help refine the empirical power laws derived by theory and correlate the resulting conductance as a function of molecular weight, grafting density and degree of hydration and further refines predictions of the conductivity profile as a function of pore-scale variations.

Recent work in the field has focused on polymers containing quaternary nitrogen functional groups, such as ammonium, imidazolium, and pyridinium. Some of these cations have shown promising hydroxide conductivities (notably guanidinium, at 84 mS/cm (12)) but the membranes continue to suffer from poor stability. Because electrolyte performance is strongly tied to the choice of cation, we are interested in determining the alkaline stability of some of these cations and considering other functional groups outside of the class of ammonium derivatives.

The guanidinium cation has been specifically investigated to determine alkaline stability at 20 °C, 60 °C, and 80 °C (Figures 5 and 6). An NMR study of a 4M solution of 1-benzyl-1,2,2,3,3-pentamethylguanidinium hydroxide in D_2O showed that degradation occurs quickly at higher temperatures, with approximately 77% degradation after 96 hours at 80 °C and approximately 50% degradation after 96 hours at 60 °C. At room temperature, the compound is more stable, degrading only 5% after 96 hours. Certainly, more stable cations are required for long term operation in AEMs.

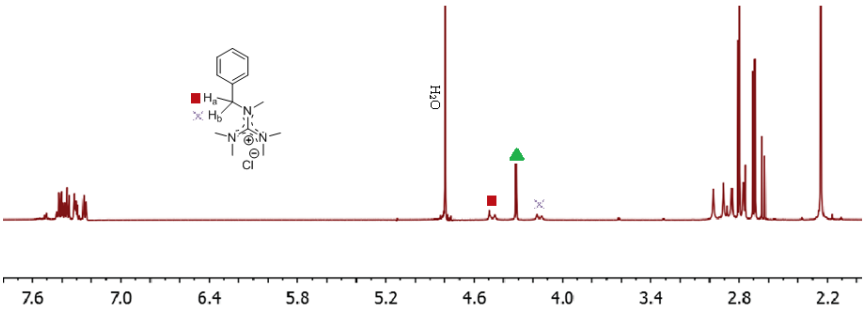

Figure 5. ^{1}H NMR of 1-benzyl-1,2,2,3,3-pentamethylguanidinium in 4M NaOH at 60 °C after 72 h. The peaks (■, 4.488 ppm) and (×, 4.1628 ppm) belong to the two protons on the methylene group of 1-benzyl-1,2,2,3,3-pentamethylguanidinium chloride. The peak (▲, 4.3071 ppm) is a new peak resulting from the decomposition of 1-benzyl-1,2,2,3,3-pentamethylguanidinium.

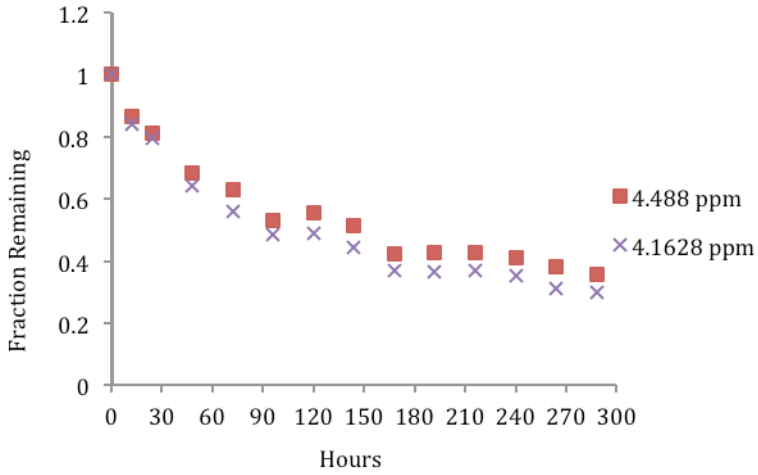

Figure 6. Degradation of 1-benzyl-1,2,2,3,3-pentamethylguanidinium chloride in 4M NaOH at 60 °C over 288 h. The curve was obtained from the integration of each peak in the ^{1}H NMR spectra measured every 24 h.

The Yan group has synthesized tris(2,4,6-trimethoxyphenyl)polysulfone-methylene quaternary-phosphonium-hydroxide (TPQPOH), a phosphonium-based hydroxide exchange membrane (HEM) (Figure 7). TPQPOH shows high conductivity (45 mS/cm (13)) and is tough, flexible, and stable in alkaline solution. The ability of TPQPOH to self-crosslink provides added control over its mechanical properties and water uptake (14). Further, it is selectively soluble in lower alcohols and other solvents so that it can be included in the catalyst layer as an ionomer, thereby extending the triple-phase boundary (15).

The performance of TPQPOH as an HEM is encouraging, but further work is required for HEMFCs to realize its full potential. Theoretical and computational contributions from Witten and Voth will elucidate the ion transport mechanisms in TPQPOH. The quaternary phosphonium cation can also be attached to the block copolymers synthesized by Coughlin and Knauss. These results will guide us as we continue our search for superior hydroxide-conducting cations.

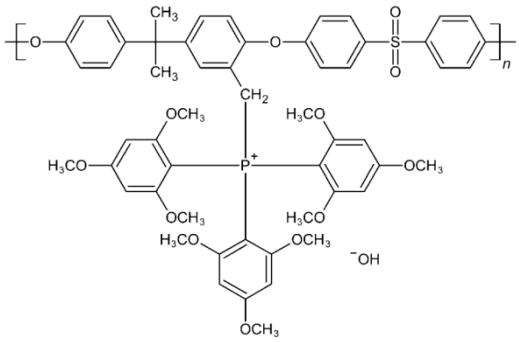

Figure 7. Structure of TPQPOH.

Measurement and Film Forming

As mentioned above, quarternary ammonium or phosphonium cations are grafted onto polymer backbones to make them conductive for applications in AEM fuel cells. We have been studying these cations and their effect on anion conductivity in solution, Figure 6. We reference complimentary stability studies at the National Renewable Energy Laboratory for the same cations both in sealed NMR tubes at elevated temperatures and computationally. Some of these cations, Figure 8, show a decrease in the conductivity at ≤80°C which can be attributed to the degradation of the cation at these increased temperatures. The CO_2 saturated solutions of these cations show almost 1.5 to 3 times drop in ionic conductivity due to the formation of carbonate and or bicarbonate anions. It was seen that amongst all the cations analyzed benzyltrimethyl ammonium cation had the maximum ionic conducivity.

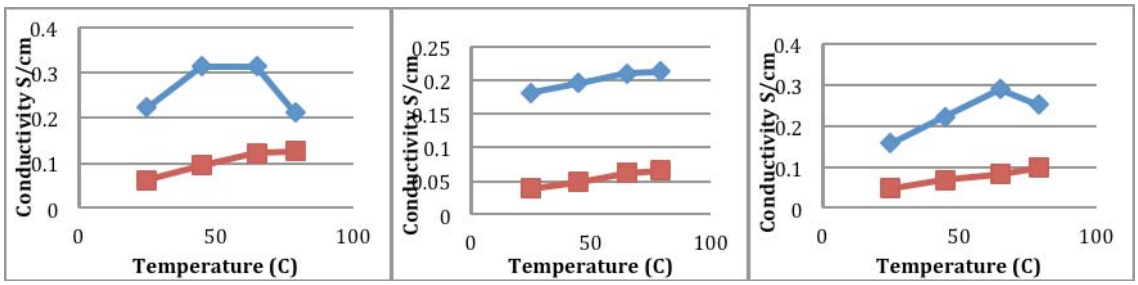

Figure 8. Ionic conductivities for hydroxide solutions, upper, under high purity nitrogen and saturated with CO_2, lower,from left to right, tetramethyl, tetraethyl and, benzyltrimethyl ammonium.

In Figure 9 is shown a cationic derivative of Nafion™. We derivatized the analogous sulfonyl fluoride version of the 3M ionomer where the side chain is-O-$(CF_2)_4$-SO_2F, with a diamine, which was further quaternized with methyl, ethyl, or butyl groups to produce a quaternary ammonium end groups.

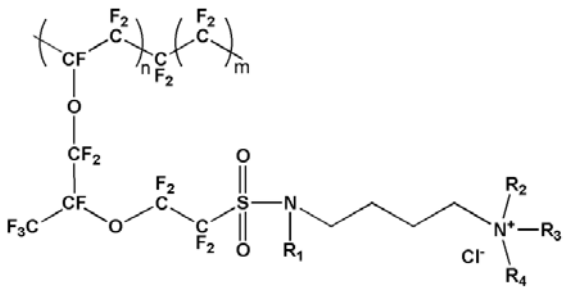

Figure 9. Cation derived version of Nafion™.

At the time of data collection we only had an ambient atmosphere environmental chamber available and so the AEMS were performed in the chloride form for base lining purposes. At 80% RH it can be seen that the tetraethyl cation clearly outperforms the tetrabutyl.

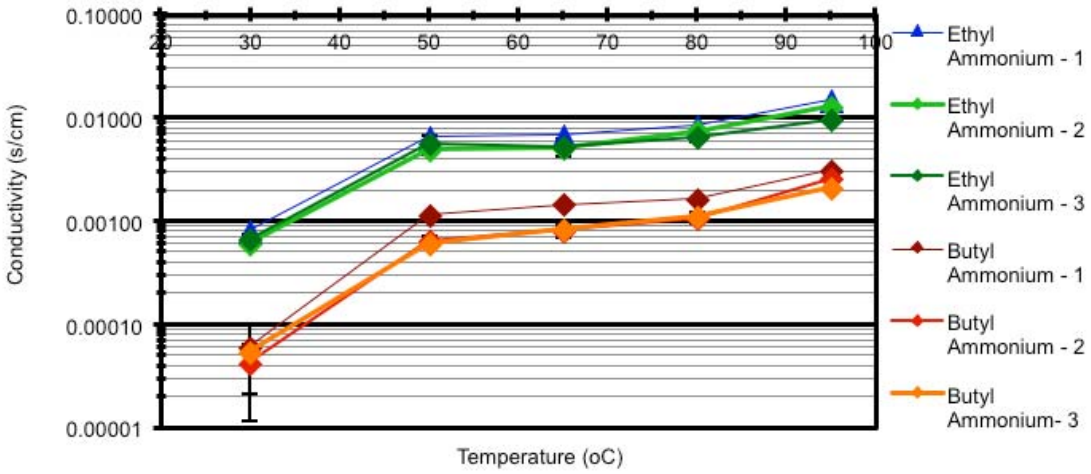

Figure 10. Ionic conductivity of AEMs in chloride form at 80%RH.

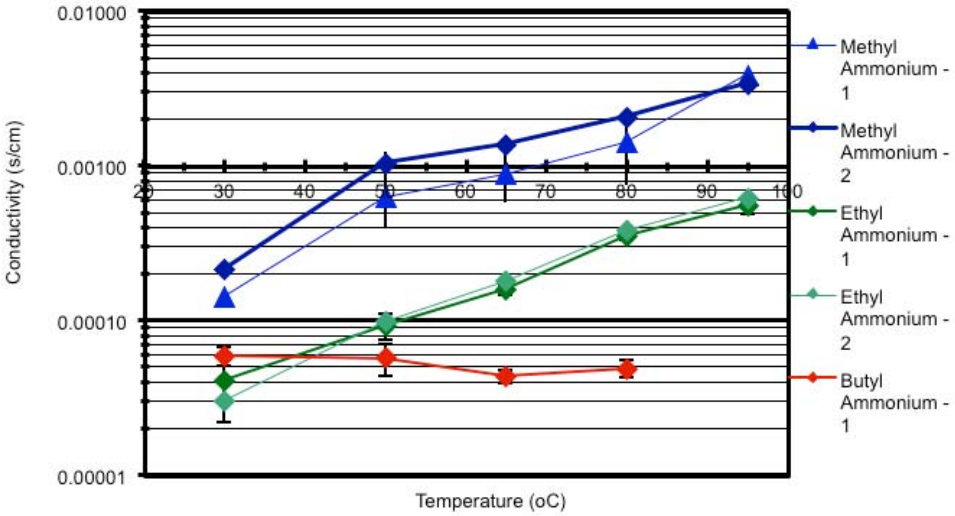

Figure 11. Ionic conductivity of AEMs originally in hydroxide form equilibrated in air at 80%RH.

When the AEMs were soaked in KOH and equilibrated in air so that the anions were exchanged to an equilibrium concentration of carbonate and bicarbonate, Figure 11, the anionic conductivities observed were an order of magnitude lower. Preliminary titration results show that samples are exchanged completely to carbonate/bicarbonate with exposure to ambient levels of carbon dioxide.

A state of the art rheometer with specialized humidity control environment is being built to perform a wide range of mechanical characterization studies on complex heterogeneous organic materials. Inertia free measurements (i.e., the ability to measure stress independently of applied strain) will be carried out on a range of polymers synthesized by the team. The complex heterogeneous organic materials will consist of polymeric solutions and films. We will be capable of characterizing the steady and oscillatory shear response, extensional, and tensile properties of the polymeric materials. Accurate and precise control at all relevant temperatures is available for these experiments. In addition, a new environmental chamber will be built to control temperature and humidity as well as quantify mechanical properties of the polymeric films under the same conditions where ion transport is quantified. The new environmental chamber will leverage Liberatore's significant experience working with TA Instruments on novel rheometer environments including two patents (16, 17) and one commercial product (a rheo-small-angle light scattering system).

Conclusions

We have begun an integrated indepth study of AEMs based on both theoretical and experimental work. Many model polymer systems have been fabricated and will be fully characterized and the results obtained applied to the theory and modeling of anion transport at multiple length scales. Bulk random AEMs are being studied to understand the limits of anion transport and film forming.

Acknowledgments

We would like to thank the ARO for funding this MURI under contract W911NF-10-1-0520. Use of the Advanced Photon Source, an Office of Science User Facility operated for the U.S. Department of Energy (DOE) Office of Science by Argonne National Laboratory, was supported by the U.S. DOE under Contract No. DE-AC02-06CH11357.

References

1. Spendelow, J. S.; Wieckowski, A., *Phys. Chem. Chem. Phys.* 2007, 9, (21), 2654-2675.
2. Varcoe, J. R.; Slade, R. C. T., *Fuel Cells* 2005, 5, (2), 187-200.
3. Marx, D.; Chandra, A.; Tuckerman, M. E. *Chem. Rev.* **2010**, *110*, 2174.

4. Knight, C.; Maupin, C. M.; Izvekov, S.; Voth, G. A. *Journal of Chemical Theory and Computation* **2010**, *6*, 3223.
5. Petersen, M. K.; Voth, G. A. *The Journal of Physical Chemistry B* **2006**, *110*, 18594.
6. Monaghan J. J. *Reports on Progress in Physics* **2005**, *68*, 1703.
7. Ayton, G. S.; McWhirter, J. L.; McMurtry, P.; Voth, G. A. *Biophysical Journal* **2005**, *88*, 3855.
8. Mauritz, K. A.; Moore, R. B., *Chemical Reviews* **2004**, *104*, 4535.
9. Lenz, M.; Witten, T. A., unpublished results.
10. S. Ochi; O. Kamishima; J. Mizusaki; and J. Kawamura, *Solid State Ionics*, **2009**, *180* 580.
11. Milner, S. T.; Witten, T. A; and Cates, M. E., *Macromolecules*, **1988**, *21*, 2610.
12. J. Wang, Z. Zhao, F. Gong, S. Li, and S. Zhang, *Macromolecules*, **2009**, *42*, 8711.
13. S. Gu, R. Cai, T. Luo, K. Jensen, C. Contreras, and Y. S. Yan, *ChemSusChem*, **2010**, *5*, 555.
14. S. Gu, R. Cai, and Y. S. Yan, *Chem. Commun.*, **2011**, *47*, 2856.
15. S. Gu, R. Cai, T. Luo, Z. Chen, M. Sun, Y. Liu, G. He, and Y. S. Yan, *Angew. Chem. Int. Ed.*, **2009**, *48*, 6363.
16. Liberatore, M.W., N.J. Wagner, and N. Doe, *System and method for improved optical measurement during rheometric measurements.* U.S. 7,594,429.
17. Liberatore, M.W., N.J. Wagner, and P. Foster, *System for in-situ optical measurement and sample heating during rheometric measurements.* U.S. 7,500,385.